

Journal of Organometallic Chemistry, 365 (1989) 325–340
 Elsevier Sequoia S.A., Lausanne – Printed in The Netherlands
 JOM 09483

Antiferromagnetic complexes with metal–metal bonds

XVIII *. The influence of electronic factors on geometry of heterometallospirane clusters. Molecular structure and magnetic properties of $\text{Cp}_2\text{Cr}_2(\mu\text{-SCMe}_3)(\mu_3\text{-S})_2\text{-M}(\mu_3\text{-S})_2\text{Fe}_2(\text{CO})_6$ ($\text{M} = \text{Fe, Rh}$) and $(\text{MeC}_5\text{H}_4)_2\text{-Cr}_2(\mu\text{-SCMe}_3)(\mu_3\text{-S})_2\text{Co}(\mu_3\text{-S})_2\text{Fe}_2(\text{CO})_6$

I.L. Eremenko, A.A. Pasynskii *, A.S. Katugin, V.R. Zalmanovitch, B. Orazsakhatov, S.A. Sleptsova, A.I. Nekhaev, V.V. Kaverin, O.G. Ellert, V.M. Novotortsev

*N.S. Kurnakov Institute of General and Inorganic Chemistry, Academy of Sciences of the USSR,
 Leninsky prosp. 31, Moscow (U.S.S.R.)*

A.I. Yanovsky, V.E. Shklover, and Yu.T. Struchkov

*A.N. Nesmeyanov Institute of Organoelement Compounds, Academy of Sciences of the USSR,
 Vavilov St., 28, Moscow (U.S.S.R.)*

(Received September 19th, 1988)

Abstract

Reaction of $\text{Cp}_2\text{Cr}_2(\text{SCMe}_3)_2\text{S}$ (I) with $\text{Fe}_3\text{S}_2(\text{CO})_9$ gives the novel metallospirane cluster $\text{Cp}_2\text{Cr}_2(\mu\text{-SCMe}_3)(\mu_3\text{-S})_2\text{Fe}(\mu_3\text{-S})_2\text{Fe}_2(\text{CO})_6$ (II). Analogous clusters with Co and Rh as central ions (III and IV respectively) have been obtained from the reaction of $(\text{MeC}_5\text{H}_4)_2\text{Cr}_2(\mu\text{-SCMe}_3)(\mu_3\text{-S})_2\text{Co}(\text{CO})_2$ or $\text{Cp}_2\text{Cr}_2(\mu\text{-SCMe}_3)(\mu_3\text{-S})_2\text{RhL}_2$ ($\text{L} = \text{CO, L}_2 = \text{COD}$) with $\text{Fe}_2(\text{CO})_6\text{S}_2$. The X-ray diffraction study of II (space group $P\bar{1}$, a 9.691(4), b 12.294(3), c 14.515(5) Å, α 66.25(2), β 74.89(3), γ 78.61(3)°, V 1519.8 Å³, $Z = 2$) reveals Cr_2Fe and Fe_3 triangles in the Cr_2FeFe_2 metallospirane core at a dihedral angle of 106.8°, and the geometry of dichromium disulfide thiolate fragment remains unchanged as compared to I, III and IV (Cr–Cr 2.689; 2.610(2); 2.598(2); 2.608(5) Å in I–IV, respectively). II has strong Cr–Fe bonds (2.717(2) and 2.727(2) Å), but the two bonds between the central and peripheral Fe atoms (3.018(2) and 3.032(2) Å) are relatively weak. The

* For part XVII see ref. 8.

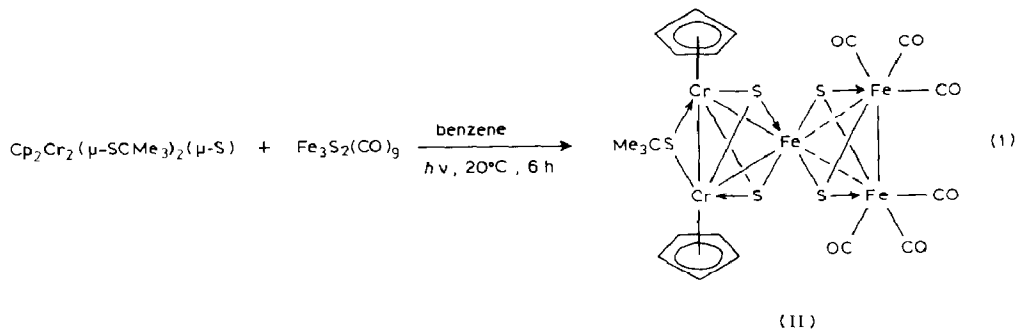
peripheral Fe–Fe bond (2.503(2) Å) is still rather short. Formal replacement of the Fe atom in II by the Co atom in III (space group *Pnam*, *a* 14.549(2), *b* 14.480(2), *c* 14.146(2) Å, *V* 2980.1 Å³, *Z* = 4) results in the rupture of the Fe–Fe bond (Fe...Fe 3.399(2) Å) and formation of the two single Co–Fe bonds (2.554 (2) and 2.538(2) Å). The dihedral angle between the planes of the metal triangles Cr₂Co and CoFe₂ in III is 90°. The geometry of the Rh(S)₂Fe₂(CO)₆ moiety in the Rh-containing metall-spirane IV (space group *P2₁/n*, *a* 9.800(2), *b* 12.983(3), *c* 22.606(5) Å, β 97.05(2)°, *V* 2854.3 Å³, *Z* = 4) is not significantly different from that of the Co(S)₂Fe₂(CO)₆ fragment in III (Rh–Fe 2.650(4) Å, Fe...Fe 3.344(4) Å), the main difference involves the dihedral angle between the Cr₂Rh and RhFe₂ planes, which is 129.1° in IV. This difference being due to the tendency of the Rh¹ atom to form the square planar complexes on one hand, and to decreasing the repulsion between the S atoms and the strengthening the Rh–Cr bonds in the nonplanar ligand environment of the Rh atom on the other.

Introduction

We have recently discussed different synthetic routes to antiferromagnetic sulfide bridged homo- and hetero-metallospirane clusters $[(RC_5H_4)_2Cr_2(\mu\text{-SCMe}_3)(\mu_3\text{-S})_2]_2M$ which were designated as Q₂M (*R* = H) or Q'₂M (*R* = Me), where M = V, Cr, Mn, Fe, Co, Ni. The geometry of the Cr₂MCr₂ core, and specifically, the Cr–M bond characteristics and the magnitude of the dihedral angle between the Cr₂M planes are sensitive to the electronic configuration of the metal atom [1]. At the same time the peripheral binuclear fragments Q (or Q') do not show any significant geometrical changes, and may be regarded as 5e ligands donating 3 electrons from two sulfur atoms and 2 electrons from the half-filled orbitals of the chromium atoms. On the other hand some cluster derivatives are known in which the Fe₂S₂(CO)₆ moiety acts as a two-, four- or six-electron ligand. In the complexes (PPh₃)₂Pd(μ_3 -S)₂Fe₂(CO)₆ [2,3] and [(CO)₆Fe₂(μ_3 -S)₂]₂Ge [4] without direct Fe–Pd or Fe–Ge bonds (Pd has a square planar and Ge has a tetrahedral ligand environment) as well as in (Cp₂V)₂(μ -S)₂Fe₂(CO)₆ [3] this group is a 2e donor. The same ligand is a 4e donor in Fe₃S₂(CO)₉ whereas in [(CO)₆Fe(μ -S)₂Fe(μ -S)₂Mo(S)₂]²⁻(Et₄N⁺)₂ it acts as a 6e-donating ligand donating 2e to the Fe^{II} electronic shell from the sulfur atoms and 4e from the two filled orbitals of the Fe^I atoms bonded to each other via a short Fe–Fe bond [5]. It was of special interest to construct new heterometallospirane clusters by combining the binuclear fragments Q and Fe₂S₂(CO)₆ to the central Fe, Co and Rh ions as ligands and to find out whether the character of the metal–metal bond involving the central and peripheral metal atoms could be predicted.

Results and discussion

The photochemical reaction of Cp₂Cr₂(μ -SCMe₃)₂(μ -S) (I) with Fe₃(μ_3 -S)₂(CO)₉ (eq. 1) gave the first metallspirane cluster of this series namely QFe(μ_3 -S)₂Fe₂(CO)₆ (II) having Fe^{III} as a central ion. II was isolated as browngreen prisms,



soluble in hydrocarbons. II is antiferromagnetic, μ_{eff} decreasing from 1.19 to 0.95 BM in the temperature range 296–80 K which is consistent with the Heisenberg–Dirak–Van Vleck (HDVV) model [6] for a symmetric trimer containing two Cr^{III} ($S = 3/2$) ions and a high-spin Fe^{III} ($S = 5/2$) ion with the exchange parameters, $-2J(\text{Cr}-\text{Cr}) 440 \text{ cm}^{-1}$ and $-2J(\text{Cr}-\text{Fe}) 630 \text{ cm}^{-1}$. The IR spectrum of II shows bands corresponding to CO stretching vibrations at 1940, 1960, 1985, 2010, 2045 cm^{-1} . The X-ray diffraction study of complex II (Fig. 1, Tables 1–3) shows that the peripheral binuclear moieties are characterized by short Cr–Cr (2.610(2) Å) and Fe–Fe (2.503(2) Å) bonds. The central Fe^{III} atom (d^5 configuration) forms four Fe–S bonds involving the μ_3 -sulfide atoms (average length 2.268(3) Å), two short Fe–Cr (2.717(2) and 2.727(2) Å) and two long Fe_(central)–Fe_(periph.) (3.018(2) and 3.032(2) Å) bonds. The analogous elongation up to 3.11 Å for the half-order bond Fe–Cr has been found previously in the triangular cluster QFe(CO)₃ [1]. The dihedral angle between the triangular fragment Cr₂Fe and Fe₃ in molecule II is 106.8° (Fig. 1).

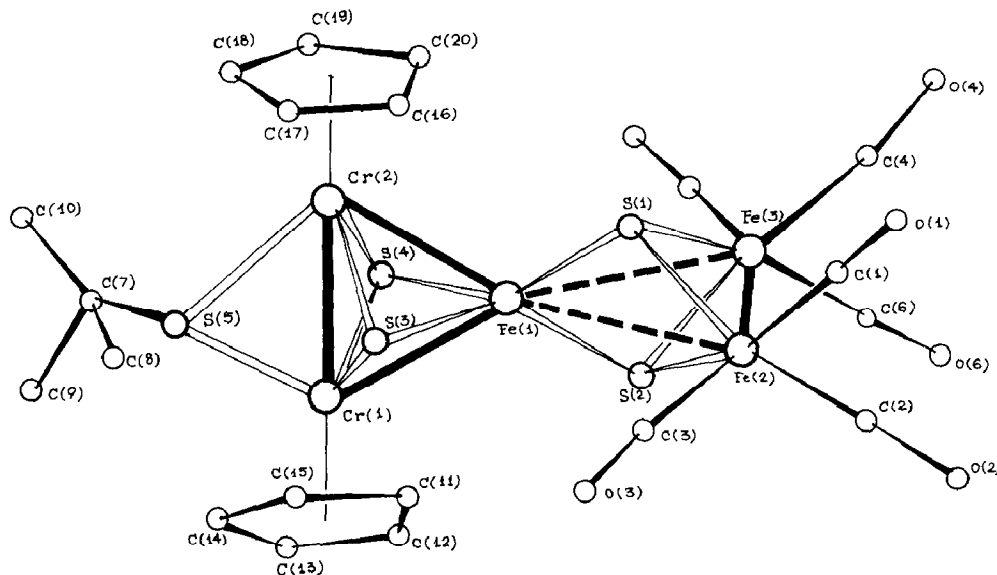


Fig. 1. The structure of $\text{Cp}_2\text{Cr}_2(\mu-\text{SCMe}_3)_2(\mu_3-\text{S})_2\text{Fe}(\mu_3-\text{S})_2\text{Fe}_2(\text{CO})_6$.

Table 1

Atomic coordinates for $(C_5H_5)_2Cr_2(\mu\text{-SCMe}_3)(\mu_3\text{-S})_2Fe(\mu_3\text{-S})_2Fe_2(CO)_6$ (II)

Atom	<i>x</i>	<i>y</i>	<i>z</i>
Fe(1)	0.27489(13)	0.81764(10)	0.86175(9)
Fe(2)	0.16186(13)	0.75880(10)	0.71399(9)
Fe(3)	0.20814(13)	0.97256(11)	0.65186(9)
Cr(1)	0.22376(14)	0.76600(11)	1.06809(10)
Cr(2)	0.58722(14)	0.78677(11)	0.96346(10)
S(1)	0.0635(2)	0.8772(2)	0.8080(2)
S(2)	0.3798(2)	0.8155(2)	0.7051(2)
S(3)	0.3491(2)	0.6440(2)	0.9839(2)
S(4)	0.3047(2)	0.9384(2)	0.9384(2)
S(5)	0.4170(2)	0.7696(2)	1.1348(2)
O(1)	-0.1039(7)	0.8122(7)	0.6358(5)
O(2)	0.3318(8)	0.6688(7)	0.5549(6)
O(3)	0.0940(8)	0.5365(6)	0.8899(5)
O(4)	0.3581(7)	0.9841(6)	0.4451(5)
O(5)	-0.0603(8)	1.1112(7)	0.5925(6)
O(6)	0.3311(10)	1.1671(7)	0.6634(8)
C(1)	-0.0006(10)	0.7922(8)	0.6668(7)
C(2)	0.2621(9)	0.7031(8)	0.6175(7)
C(3)	0.1281(10)	0.6204(8)	0.8200(7)
C(4)	0.2991(10)	0.9830(8)	0.5243(7)
C(5)	0.0464(11)	1.0581(9)	0.6143(8)
C(6)	0.2831(12)	1.0894(9)	0.6608(8)
C(7)	0.4814(10)	0.6291(8)	1.2340(7)
C(8)	0.6439(10)	0.6333(9)	1.2215(8)
C(9)	0.4060(13)	0.6377(11)	1.3380(8)
C(10)	0.4543(12)	0.5175(8)	1.2225(8)
C(11)	-0.0082(9)	0.8311(8)	1.0746(8)
C(12)	0.0316(10)	0.8366(9)	1.1600(8)
C(13)	0.0754(10)	0.7187(10)	1.2213(7)
C(14)	0.0632(9)	0.6412(8)	1.1751(7)
C(15)	0.0103(10)	0.7099(8)	1.0851(7)
C(16)	0.6621(9)	0.9052(7)	0.8809(7)
C(17)	0.7123(9)	0.8059(8)	0.9612(7)
C(18)	0.7120(9)	0.7016(8)	0.9413(7)
C(19)	0.6640(10)	0.7362(8)	0.8495(7)
C(20)	0.6336(9)	0.8632(8)	0.8109(7)

Quite a different situation is observed in the cluster $Q'\text{Co}(\mu_3\text{-S})_2\text{Fe}_2(\text{CO})_6$ (III) which is the product of the formal replacement of the Fe atom in II by the Co atom. Complex III was obtained as relatively air-stable, brown crystals according to:

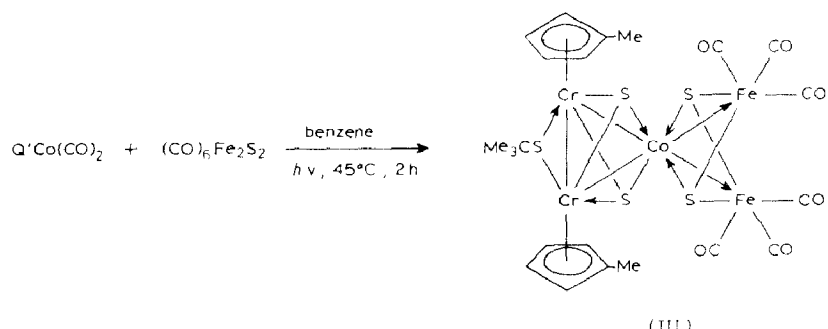


Table 2

Bond distances (\AA) in $(\text{C}_5\text{H}_5)_2\text{Cr}_2(\mu\text{-SCMe}_3)(\mu_3\text{-S})_2\text{Fe}(\mu_3\text{-S})_2\text{Fe}_2(\text{CO})_6$ (II)

Bond	<i>d</i>	Bond	<i>d</i>	Bond	<i>d</i>
Fe(1)–Fe(2)	3.018(2)	Fe(1)–Fe(3)	3.032(2)	Fe(1)–Cr(1)	2.727(2)
Fe(1)–Cr(2)	2.717(2)	Fe(2)–S(1)	2.263(3)	Fe(1)–S(2)	2.245(2)
Fe(1)–S(3)	2.286(3)	Fe(1)–S(4)	2.278(3)	Fe(2)–Fe(3)	2.503(2)
Fe(2)–S(1)	2.295(3)	Fe(2)–S(2)	2.309(3)	Fe(2)–C(1)	1.79(1)
Fe(2)–C(2)	1.78(1)	Fe(2)–C(3)	1.794(9)	Fe(3)–S(2)	2.301(3)
Fe(3)–S(1)	2.308(3)	Fe(3)–C(4)	1.796(9)	Fe(3)–C(5)	1.79(1)
Fe(3)–C(6)	1.79(1)	Cr(1)–Cr(2)	2.610(2)	Cr(1)–S(3)	2.281(3)
Cr(1)–S(4)	2.307(3)	Cr(1)–S(5)	2.336(3)	Cr(2)–S(4)	2.285(3)
Cr(2)–S(3)	2.294(3)	Cr(2)–S(5)	2.333(2)	S(5)–C(7)	1.87(1)
C(7)–C(8)	1.55(2)	C(7)–C(9)	1.53(2)	C(7)–C(10)	1.53(2)
C(1)–O(1)	1.15(1)	C(2)–O(2)	1.16(1)	C(3)–O(3)	1.15(1)
C(4)–O(4)	1.14(1)	C(5)–O(5)	1.15(1)	C(6)–O(6)	1.16(2)

Although the cyclopentadienyl analogue was obtained similarly, it proved impossible to grow suitable crystals for the X-ray diffraction study. The four bands assigned to the CO stretching vibrations 1960, 1970, 2015, 2050 cm^{-1} are present in the IR spectrum of III. In contrast to the paramagnetic central Fe^{III} ion in II, Co^{I} in III is diamagnetic which is reflected in the magnetic properties of III (consistent with the HDVV dimeric model [6] ($-2J = 502 \text{ cm}^{-1}$) μ_{eff} per one Cr atom decreases from 1.27 to 0.89 BM in the temperature range 291–77 K). The X-ray diffraction study (Fig. 2, 3; Tables 4–6) showed that the dichromium fragment of the cluster has the same geometry as in II (Cr–Cr 2.598(2) \AA) but III has strong Cr–Co (2.629(1) \AA) and S–Co (2.182(2)–2.198(2) \AA) bonds. On the other hand III has two short Co–Fe bonds (2.538(2) and 2.554(2) \AA), whereas the Fe...Fe distance 3.399(2) \AA is non-bonding, the dihedral angle between the planes of the Cr_2Co and CoFe_2 triangles is 90° .

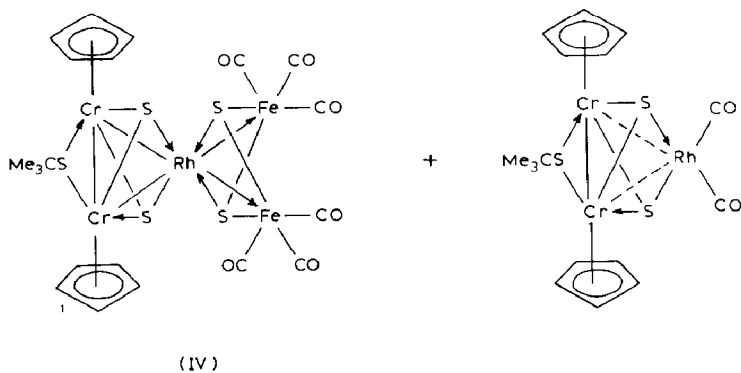
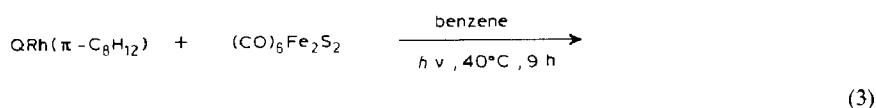


Table 3

Bond angles (degrees) in $(C_5H_5)_2Cr_2(\mu\text{-SCMe}_3)(\mu_3\text{-S})_2Fe(\mu_3\text{-S})_2Fe_2(CO)_6$ (II)

Angle	ω	Angle	ω
Fe(2)Fe(1)Fe(3)	48.88(4)	Fe(2)Fe(1)Cr(1)	137.99(6)
Fe(2)Fe(1)Cr(2)	149.04(6)	Fe(2)Fe(1)S(1)	49.98(7)
Fe(2)Fe(1)S(2)	49.40(7)	Fe(2)Fe(1)S(3)	109.17(8)
Fe(2)Fe(1)S(4)	154.82(8)	Fe(3)Fe(1)Cr(1)	149.89(6)
Fe(3)Fe(1)Cr(2)	136.89(6)	Fe(3)Fe(1)S(1)	49.09(7)
Fe(3)Fe(1)S(2)	48.95(7)	Fe(3)Fe(1)S(3)	154.93(8)
Fe(3)Fe(1)S(4)	108.69(8)	Cr(1)Fe(1)Cr(2)	57.30(5)
Cr(1)Fe(1)S(1)	109.07(8)	Cr(1)Fe(1)S(2)	160.93(9)
Cr(1)Fe(1)S(3)	53.25(7)	Cr(1)Fe(1)S(4)	54.00(7)
Cr(2)Fe(1)S(1)	161.93(9)	Cr(2)Fe(1)S(2)	107.55(8)
Cr(2)Fe(1)S(3)	53.76(7)	Cr(2)Fe(1)S(4)	53.58(7)
S(1)Fe(1)S(2)	88.04(9)	S(1)Fe(1)S(3)	130.37(10)
S(1)Fe(1)S(4)	109.5(1)	S(2)Fe(1)S(3)	109.3(1)
S(2)Fe(1)S(4)	129.1(1)	S(3)Fe(1)S(4)	95.02(9)
Fe(1)Fe(2)Fe(3)	65.85(2)	Fe(1)Fe(2)S(1)	48.07(7)
Fe(1)F(2)S(2)	47.59(7)	Fe(1)Fe(2)C(1)	137.1(3)
Fe(1)Fe(2)C(2)	127.9(3)	Fe(1)Fe(2)C(3)	84.4(3)
Fe(3)Fe(2)S(1)	57.32(7)	Fe(3)Fe(2)S(2)	56.96(7)
Fe(3)Fe(2)C(1)	94.8(3)	Fe(3)Fe(2)C(2)	106.7(3)
Fe(3)Fe(2)C(3)	148.4(3)	S(1)Fe(2)S(2)	85.76(9)
S(1)Fe(2)C(1)	89.1(3)	S(1)Fe(2)C(2)	164.0(3)
S(1)Fe(2)C(3)	95.2(3)	S(2)Fe(2)C(1)	148.9(3)
S(2)Fe(2)C(2)	83.8(3)	S(2)Fe(2)C(3)	110.5(3)
C(1)Fe(2)C(2)	93.6(5)	C(1)Fe(2)C(3)	100.5(5)
C(2)Fe(2)C(3)	99.8(4)	Fe(1)Fe(3)Fe(2)	65.27(5)
Fe(1)Fe(3)S(1)	47.80(7)	Fe(1)Fe(3)S(2)	47.38(7)
Fe(1)Fe(3)C(4)	132.3(3)	Fe(1)Fe(3)C(5)	131.4(4)
Fe(1)Fe(3)C(6)	86.8(4)	Fe(2)Fe(3)S(1)	56.79(7)
Fe(2)Fe(3)S(2)	57.26(7)	Fe(2)Fe(3)C(4)	95.6(3)
Fe(2)Fe(3)C(5)	105.3(4)	Fe(2)Fe(3)C(6)	151.5(4)
S(1)Fe(3)S(2)	85.63(9)	Fe(1)S(1)Fe(2)	82.95(9)
Fe(1)S(1)Fe(3)	83.11(9)	Fe(2)S(1)Fe(3)	65.89(8)
Fe(1)Cr(1)Cr(2)	61.15(5)	Fe(1)Cr(1)S(3)	54.41(7)
Fe(1)Cr(1)S(4)	53.02(7)	Fe(1)Cr(1)S(5)	116.54(8)
Cr(2)Cr(1)S(3)	55.45(7)	Cr(2)Cr(1)S(4)	54.97(7)
Cr(2)Cr(1)S(5)	55.95(7)	S(3)Cr(1)S(4)	94.36(9)
S(3)Cr(1)S(5)	94.48(9)	S(4)Cr(1)S(5)	83.59(9)
Fe(1)Cr(2)Cr(1)	61.55(5)	Fe(1)Cr(2)S(3)	53.47(7)
Fe(1)Cr(2)S(4)	53.34(7)	Fe(1)Cr(2)S(5)	117.06(8)
Cr(1)Cr(2)S(3)	54.97(7)	Cr(1)Cr(2)S(4)	55.76(7)
Cr(1)Cr(2)S(5)	56.08(7)	S(3)Cr(2)S(4)	94.60(9)
S(3)Cr(2)S(5)	94.22(9)	S(4)Cr(2)S(5)	84.16(9)
Fe(1)S(3)Cr(1)	73.34(8)	Fe(1)S(3)Cr(2)	72.77(8)
Cr(1)S(3)Cr(2)	69.58(8)	Fe(1)S(2)Fe(2)	83.02(9)
Fe(1)S(2)Fe(3)	83.67(9)	Fe(2)S(2)Fe(3)	65.79(8)
Fe(1)S(4)Cr(1)	72.99(8)	Fe(1)S(4)Cr(2)	73.08(8)
Cr(1)S(4)Cr(2)	69.27(8)	Cr(1)S(5)Cr(2)	67.98(8)

Metallospirane $QRh(\mu_3\text{-S})_2Fe_2(CO)_6$ (IV) with the Rh central atom is formed by the reaction 3.

Complex IV was isolated as air-stable, brown prisms. The IR spectrum of IV is

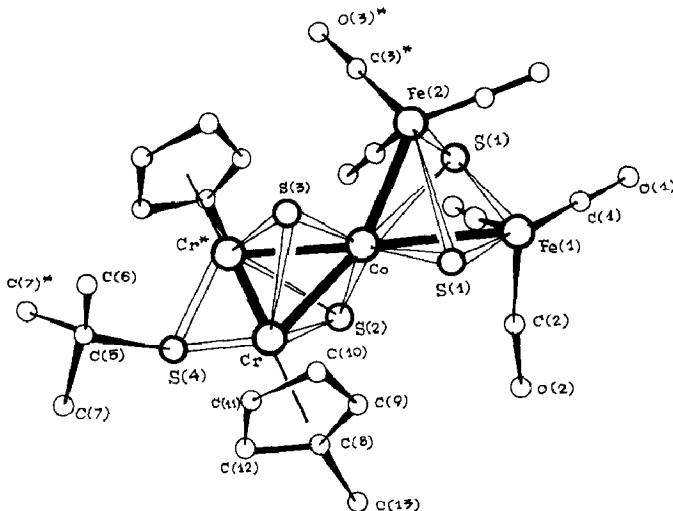


Fig. 2. The structure of $(\text{MeC}_5\text{H}_4)_2\text{Cr}_2(\mu\text{-SCMe}_3)(\mu_3\text{-S})_2\text{Co}(\mu_3\text{-S})_2\text{Fe}_2(\text{CO})_6$.

similar to that of III with the four bands assigned to the CO stretching vibrations at 1955, 1995, 2020 and 2050 cm^{-1} . The central Rh^{l} ion is diamagnetic whereas complex IV is antiferromagnetic: $\mu_{\text{eff}}/\text{Cr}$ atom decreasing from 1.25 BM to 0.86 MB in the temperature range 296–77 K, which corresponds to an exchange parameter in the dichromium fragment of $-2J = 427 \text{ cm}^{-1}$. It is noteworthy that the geometry of IV (Fig. 4, Tables 7–9) differs strongly from that of III. The dihedral angle between the triangles Cr_2Rh and RhFe_2 (129.1°) is much larger than analogous dihedral angle in III (90°). Strong Cr–Rh bonds (2.720(4) and 2.724(4) Å) exist in the triangular fragment QRh (with the Cr–Cr bond length of 2.608(5) Å). Similar Cr–Rh distances (2.757 Å) were found in $\text{C}_6\text{H}_6\text{CrRh}(\text{Me}_5\text{C}_5)(\text{CO})_2(\mu\text{-CO})_2$

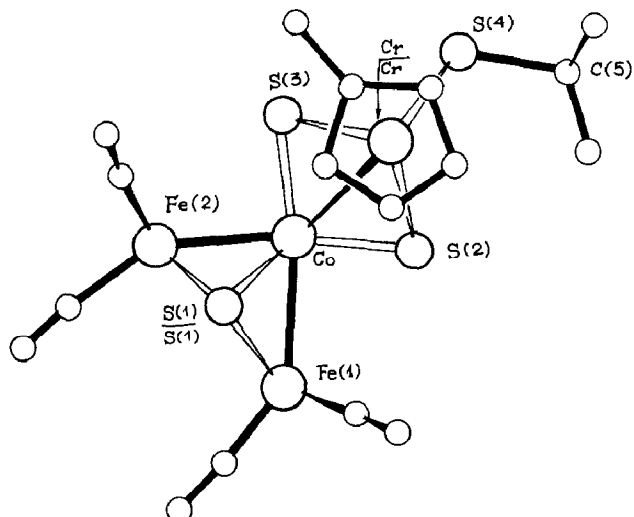


Fig. 3. Projection of molecule $(\text{MeC}_5\text{H}_4)_2\text{Cr}_2(\mu\text{-SCMe}_3)(\mu_3\text{-S})_2\text{Co}(\mu_3\text{-S})_2\text{Fe}_2(\text{CO})_6$ along the Cr–Cr axis.

Table 4

Atomic coordinates and the isotropic equivalent parameters for $(\text{MeC}_5\text{H}_4)_2\text{Cr}_2(\mu\text{-SCMe}_3)(\mu_3\text{-S})_2\text{Co}(\mu_3\text{-S})_2\text{Fe}_2(\text{CO})_6$ (III)

Atom	<i>x</i>	<i>y</i>	<i>z</i>	B_{eq}^{a}
Co	0.68471(9)	0.06269(8)	0.750	2.53(3)
Fe(1)	0.7798(1)	-0.0843(1)	0.750	3.43(3)
Fe(2)	0.5488(1)	-0.0489(1)	0.750	3.59(3)
Cr	0.70669(7)	0.21900(7)	0.65818(8)	2.38(2)
S(1)	0.6667(1)	-0.0498(1)	0.8527(1)	3.36(4)
S(2)	0.8117(2)	0.1438(2)	0.750	2.81(5)
S(3)	0.5852(2)	0.1755(2)	0.750	2.60(5)
S(4)	0.7439(2)	0.3478(2)	0.750	2.67(5)
O(1)	0.9164(4)	-0.0552(4)	0.8982(5)	6.5(2)
O(2)	0.7709(8)	-0.2858(5)	0.750	10.4(4)
O(3)	0.4287(4)	0.0183(5)	0.9008(5)	7.1(20)
O(4)	0.5059(7)	-0.2466(6)	0.750	10.0(4)
C(1)	0.8619(5)	-0.0674(5)	0.8403(6)	4.3(2)
C(2)	0.7743(9)	-0.2090(9)	0.750	6.3(4)
C(3)	0.4747(5)	-0.0084(6)	0.8413(6)	4.3(2)
C(4)	0.5204(9)	-0.1689(9)	0.750	6.2(4)
C(5)	0.6566(7)	0.4447(6)	0.750	3.5(2)
C(6)	0.5572(7)	0.4077(7)	0.750	4.5(3)
C(7)	0.6758(6)	0.5019(5)	0.8397(6)	4.7(2)
C(8)	0.7937(5)	0.2197(6)	0.5266(5)	4.0(2)
C(9)	0.7377(5)	0.3004(5)	0.5290(5)	3.8(2)
C(10)	0.6443(5)	0.2720(6)	0.5259(5)	4.2(2)
C(11)	0.6416(5)	0.1751(5)	0.5234(5)	4.2(2)
C(12)	0.7328(6)	0.1416(5)	0.5230(5)	4.4(2)
C(13)	0.8975(6)	0.2178(7)	0.5235(7)	6.2(2)

^a Anisotropically refined atoms are given in the form of the isotropic equivalent displacement parameter defined as: $4/3[a^2B_{11} + b^2B_{22} + c^2B_{33} + ab(\cos \gamma)B_{12} + ac(\cos \beta)B_{13} + bc(\cos \alpha)B_{23}]$.

Table 5

Bond distances (\AA) in $(\text{MeC}_5\text{H}_4)_2\text{Cr}_2(\mu\text{-SCMe}_3)(\mu_3\text{-S})_2\text{Co}(\mu_3\text{-S})_2\text{Fe}_2(\text{CO})_6$ (III)

Bond	<i>d</i>	Bond	<i>d</i>
Co–Fe(1)	2.538(2)	Cr–S(4)	2.336(2)
Co–Fe(2)	2.554(2)	S(4)–C(5)	1.893(8)
Co–Cr	2.629(1)	O(1)–C(1)	1.154(8)
Co–S(1)	2.198(2)	O(2)–C(2)	1.11(1)
Co–S(2)	2.189(2)	O(3)–C(3)	1.142(8)
Co–S(3)	2.182(2)	O(4)–C(4)	1.14(1)
Fe(1)–S(1)	2.250(2)	C(5)–C(6)	1.54(1)
Fe(1)–C(1)	1.767(8)	C(5)–C(7)	1.541(8)
Fe(1)–C(2)	1.81(1)	C(8)–C(9)	1.426(8)
Fe(2)–S(1)	2.248(2)	C(8)–C(12)	1.438(9)
Fe(2)–C(3)	1.781(8)	C(8)–C(13)	1.510(9)
Fe(2)–C(4)	1.79(1)	C(9)–C(10)	1.420(8)
Cr–Cr	2.598(2)	C(10)–C(11)	1.405(9)
Cr–S(2)	2.281(2)	C(11)–C(12)	1.413(9)
Cr–S(3)	2.282(2)		

Table 6

Bond angles (degrees) in $(\text{MeC}_5\text{H}_4)_2\text{Cr}_2(\mu-\text{SCMe}_3)(\mu_3-\text{S})_2\text{Co}(\mu_3-\text{S})_2\text{Fe}_2(\text{CO})_6$ (III)

Angle	ω	Angle	ω
Fe(1)CoFe(2)	83.77(6)	S(1)'Fe(2)C(3)	158.8(2)
Fe(1)CoCr	130.96(4)	S(1)Fe(2)C(4)	99.8(3)
Fe(1)CoS(1)	56.19(5)	S(1)Fe(2)C(3)	158.8(2)
Fe(1)CoS(2)	89.44(7)	S(1)'Fe(2)C(3)	89.7(2)
Fe(1)CoS(3)	171.46(8)	C(3)Fe(2)C(3)'	93.0(4)
Fe(2)CoCr	129.71(4)	C(3)Fe(2)C(4)	100.4(3)
Fe(2)CoS(1)	55.85(5)	CoCrCr	60.39(2)
Fe(2)CoS(2)	173.22(8)	CoCrS(2)	52.37(6)
Fe(2)CoS(3)	87.69(7)	CoCrS(3)	52.18(6)
CrCoCr	59.21(4)	CoCrS(4)	116.14(4)
CrCoS(1)	168.22(5)	CrCrS(2)	55.29(4)
CrCoS(2)	55.62(6)	CrCrS(3)	55.31(4)
CrCoS(3)	55.70(5)	CrCrS(4)	56.22(3)
CrCoS(1)'	109.04(5)	S(2)CrS(3)	93.59(7)
S(1)CoS(1)	82.70(9)	S(2)CrS(4)	84.80(7)
S(1)CoS(2)	119.90(6)	S(3)CrS(4)	94.78(6)
S(1)CoS(3)	118.40(6)	CoS(1)Fe(1)	69.56(6)
S(2)CoS(3)	99.10(8)	CoS(1)Fe(2)	70.11(6)
CoFe(1)S(1)	54.25(5)	Fe(1)S(1)Fe(2)	98.18(8)
CoFe(1)C(1)	104.6(2)	CoS(2)Cr	72.02(6)
CoFe(1)C(2)	144.5(4)	CrS(2)Cr	69.42(7)
S(1)Fe(1)S(1)'	80.38(9)	CoS(3)Cr	72.12(6)
S(1)Fe(1)C(1)	89.8(2)	CrS(3)Cr	69.38(8)
S(1)'Fe(1)C(1)	158.5(2)	CrS(4)Cr	67.57(7)
S(1)Fe(1)C(2)	100.9(3)	CrS(4)C(5)	115.9(2)
C(1)Fe(1)C(1)'	92.6(4)	Fe(1)C(1)O(1)	178.7(5)
C(1)Fe(1)C(2)	99.7(3)	Fe(1)C(2)O(2)	181 (2)
CoFe(2)S(1)	54.03(5)	Fe(2)C(3)O(3)	178.6(6)
CoFe(2)C(3)	105.1(2)	Fe(2)C(4)O(4)	177(2)
CoFe(2)C(4)	142.6(4)	S(4)C(5)C(6)	111.8(5)
S(1)Fe(2)S(1)'	80.5(1)	S(4)C(5)C(7)	106.1(4)
S(1)Fe(2)C(3)	89.7(2)	C(6)C(5)C(7)	110.9(5)

[7], however the Rh–Cr distances are much longer ($\sim 3.0 \text{ \AA}$) in the recently reported structures of the triangular clusters QRhL_2 ($\text{L}_2 = \pi\text{-C}_8\text{H}_{12}$ or $(\text{CO})_2$ [8]) having square-planar coordination of the Rh^{I} atom. The difersulfide moiety in IV forms two strong Rh–Fe (2.650(4) \AA) and Rh–S (2.272(6)–2.294(6) \AA) bonds, but just as in III, the Fe...Fe distance (Fe...Fe 3.344(4) \AA) is non-bonding. It is noteworthy that the triangular cluster $\text{QRh}(\text{CO})_2$, previously reported [8], is always formed along with complex IV. It may mean that $(\text{CO})_6\text{Fe}_2\text{S}_2$ carbonylates the initial $\text{QRh}(\text{C}_8\text{H}_{12})$.

In contrast to earlier reported metallospiranes Q_2M and $\text{Q}'_2\text{M}$ previously described [1], strong bonding of the five-electron fragment Q is characteristic of all the clusters of the new metallospirane series although the central metal ions (Fe^{III} , Co^{I} , Rh^{I}) have different electronic configurations and coordination abilities (Table 10). In addition cluster III, with a methylated cyclopentadienyl ring and short Cr–Cr (2.598(2) \AA) and Cr–Co (2.629(1) \AA) bonds, has the $\text{C}_5\text{H}_4\text{CH}_3$ rings in eclipsed conformation, in contrast to the staggered conformation of $\text{Q}'\text{Co}(\text{CO})_2$, $\text{Q}'_2\text{Mn}$ and $\text{Q}'_2\text{Fe}$ [1].

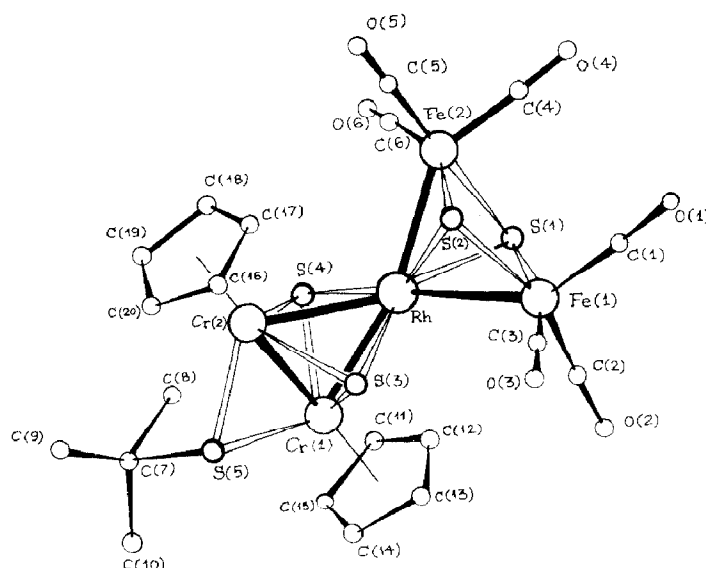
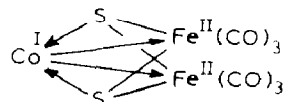


Fig. 4. The structure of $\text{Cp}_2\text{Cr}_2(\mu\text{-SCMe}_3)(\mu_3\text{-S})_2\text{Rh}(\mu_3\text{-S})_2\text{Fe}_2(\text{CO})_6$.

In complex II, the $\text{S}_2\text{Fe}_2(\text{CO})_6$ moiety is a 6e donating ligand coordinated to the Fe atom, similar to the dianion $[(\text{CO})_6\text{Fe}_2(\mu\text{-S})_2\text{Fe}(\mu\text{-S})_2\text{MoS}_2]^{2-}$ [5]. The half-filled orbitals of the central Fe^{III} ion overlap with the filled orbitals of the peripheral Fe^{I} ions thus forming half-order $\text{Fe}_{\text{(central)}}\text{-Fe}_{\text{(peripheral)}}$ bonds ($3.018(2)$ – $3.032(2)$ Å) and retaining the strong Fe–Fe bond ($2.503(2)$ Å) in the peripheral fragment.

In complex III, the $\text{Fe}_2\text{S}_2(\text{CO})_6$ group has lost its S–S and Fe–Fe bond and so becomes 4e donor. The Fe^{I} atoms can be oxidized to Fe^{II} which are not bonded to each other ($\text{Fe}\dots\text{Fe}$ $3.399(2)$ Å), but form strong bonds with the Co^{I} atom ($2.538(2)$, $2.554(2)$ Å) as indicated:



The Co–Fe bond lengths are approximately the same as in the 48e triangular cluster $(\text{CO})_9\text{Co}_2\text{FeS}$ (2.550 – 2.556 Å) [9].

Similarly the $(\text{CO})_6\text{Fe}_2(\text{S})_2$ group has the strong Rh–Fe bonds ($2.650(4)$ Å) but lacks the Fe–Fe interaction ($\text{Fe}\dots\text{Fe}$ $3.344(4)$ Å) in the rhodium-containing spirane IV. We have mentioned that the main difference between the latter and its Co analogue III is the smaller dihedral angle between the planes of the Cr_2M and MFe_2 triangles in III (90°) as opposed to 129.1° in IV. However the Rh atom in IV does not take on the square-planar environment observed in $\text{QRh}(\text{CO})_2$ and $\text{QRh}(\text{C}_8\text{H}_{12})$ [8].

Apparently the repulsion between the four coplanar S atoms prevents the typical for Rh^{I} square-planar coordination. On the other hand the twist of the planes of the Cr_2Rh triangles is accompanied by the significant strengthening of the Cr–Rh bond compared with $\text{QRh}(\text{CO})_2$ and $\text{QRh}(\text{C}_8\text{H}_{12})$. The optimum conformation of the molecular means a dihedral angle of 129.1° .

Table 7

Atomic coordinates and the isotropic equivalent parameters for $(C_5H_5)_2Cr_2(\mu\text{-SCME}_3)(\mu_3\text{-S})_2Rh(\mu_3\text{-S})_2Fe_2(CO)_6$ (IV)

Atom	<i>x</i>	<i>y</i>	<i>z</i>	B_{eq} ^a
Rh	0.9119(2)	0.1699(2)	0.63684(7)	2.38(3)
Fe(1)	1.0029(4)	0.2771(3)	0.5499(1)	3.61(8)
Fe(2)	0.7659(4)	0.0906(3)	0.5412(2)	3.73(8)
Cr(1)	0.8122(4)	0.1583(4)	0.7440(2)	4.2(1)
Cr(2)	1.0770(4)	0.1436(4)	0.7416(2)	5.1(1)
S(1)	0.7792(6)	0.2586(5)	0.5631(3)	3.5(1)
S(2)	0.9951(6)	0.1057(5)	0.5545(3)	3.1(1)
S(3)	0.9480(7)	0.2838(6)	0.7141(3)	4.5(2)
S(4)	0.9187(7)	0.0306(6)	0.6980(3)	5.0(2)
S(5)	0.9801(1)	0.1864(9)	0.8303(4)	8.8(3)
O(1)	0.967(2)	0.287(2)	0.4194(8)	7.7(6)
O(2)	1.302(2)	0.286(2)	0.573(1)	9.1(7)
O(3)	0.985(2)	0.490(2)	0.591(1)	9.7(7)
O(4)	0.782(2)	-0.134(1)	0.567(1)	8.0(6)
O(5)	0.475(2)	0.092(2)	0.559(1)	10.4(7)
O(6)	0.729(2)	0.090(2)	0.4117(9)	8.2(6)
C(1)	0.984(3)	0.289(2)	0.474(1)	5.5(7)
C(2)	1.181(3)	0.279(2)	0.564(1)	6.1(8)
C(3)	0.989(3)	0.407(2)	0.573(1)	6.2(7)
C(4)	0.769(3)	-0.055(2)	0.558(1)	4.7(7)
C(5)	0.588(3)	0.093(2)	0.554(1)	5.1(7)
C(6)	0.744(3)	0.090(2)	0.461(1)	6.2(8)
C(7)	0.982(3)	0.093(3)	0.889(1)	7.3(9)
C(8)	1.127(3)	0.093(3)	0.926(1)	6.9(9)
C(9)	0.958(3)	0.030(3)	0.830(1)	13.5(8)
C(10)	0.874(3)	0.104(3)	0.925(1)	7.3(9)
C(11)	0.601(3)	0.096(2)	0.715(1)	6.2(8)
C(12)	0.611(2)	0.197(2)	0.694(1)	4.0(6)
C(13)	0.631(3)	0.264(2)	0.745(1)	5.8(8)
C(14)	0.647(3)	0.196(3)	0.797(1)	7.0(9)
C(15)	0.630(2)	0.087(3)	0.779(1)	8(1)
C(16)	1.269(2)	0.221(3)	0.721(1)	8(1)
C(17)	1.249(2)	0.124(3)	0.689(1)	6.3(8)
C(18)	1.252(3)	0.037(3)	0.725(1)	8(1)
C(19)	1.279(3)	0.085(3)	0.785(1)	7.4(9)
C(20)	1.285(2)	0.192(3)	0.784(1)	8(1)

^a Anisotropically refined atoms are given in terms of the isotropic equivalent displacement parameter: $4/3[a^2B_{11} + b^2B_{22} + c^2B_{33} + ab(\cos \gamma)B_{12} + ac(\cos \beta)B_{13} + bc(\cos \alpha)B_{23}]$.

The molecular packing in crystal IV in contrast to that in III is characterized by intermolecular via contacts the CO groups of neighbouring molecules (2.940–3.152 Å). However, the intermolecular contacts in crystals of III and IV have no significant influence on the molecular packing and hence on the spirane geometry (Table 11). In contrast, the more asymmetric structure of IV leads to the more pronounced anisotropic intermolecular interactions and thus the molecular packings in crystals III and IV are changed.

Table 8

Bond distances (\AA) in $(\text{C}_5\text{H}_5)_2\text{Cr}_2(\mu\text{-SCMe}_3)(\mu_3\text{-S})_2\text{Rh}(\mu_3\text{-S})_2\text{Fe}_2(\text{CO})_6$ (IV)

Bond	<i>d</i>	Bond	<i>d</i>
Rh-Fe(1)	2.650(4)	Cr(2)-S(5)	2.39(2)
Rh-Fe(2)	2.650(4)	S(5)-C(7)	1.79(3)
Rh-Cr(1)	2.724(4)	Fe(2)-S(2)	2.238(7)
Rh-Cr(2)	2.721(4)	Fe(2)-C(4)	1.93(3)
Rh-S(1)	2.294(6)	Fe(2)-C(5)	1.81(3)
Rh-S(2)	2.280(6)	Fe(2)-C(6)	1.79(3)
Rh-S(3)	2.282(7)	Cr(1)-Cr(2)	2.608(5)
Rh-S(4)	2.272(8)	Cr(1)-S(3)	2.259(9)
Fe(1)-S(1)	2.261(7)	Cr(1)-S(4)	2.276(9)
Fe(1)-S(2)	2.230(7)	Cr(1)-S(5)	2.42(1)
Fe(1)-C(1)	1.71(3)	Cr(2)-S(3)	2.259(9)
Fe(1)-C(2)	1.74(3)	Cr(2)-S(4)	2.270(8)
Fe(1)-C(3)	1.78(3)	C-O _(cv)	1.14(3)
Fe(2)-S(1)	2.237(8)		

Experimental

All operations, preparation of the initial compounds, and synthesis of the clusters II-IV, were carried out under pure argon in absolute solvents. The initial compounds I, Ia, $(\text{CO})_6\text{Fe}_2\text{S}_2$, $(\text{CO})_9\text{Fe}_3\text{S}_2$ and $(\text{MeC}_5\text{H}_4)_2\text{Cr}_2(\mu\text{-SCMe}_3)(\mu_3\text{-S})_2\text{Co}(\text{CO})_2$ were synthesized by published methods [10-13]. IR spectra were recorded on a Specord IR-75 spectrometer in KBr pellets. Magnetic susceptibility was measured by the Faraday method by use of a device designed in the Institute of General and Inorganic Chemistry [14]. X-ray data for cluster II were obtained with a Hilger & Watts four-circle automatic diffractometer ($\lambda(\text{Mo-}K_{\alpha})$, $\theta/2\theta$ -scan), and for the clusters III and IV with a CAD4 diffractometer ($\lambda(\text{Mo-}K_{\alpha})$, the scan rate ratio ω/θ 6/5, $\theta \leq 26^\circ$) was used. (Crystal data are listed in Table 12). The structures II-IV were solved by direct methods and refined anisotropically by full-matrix least squares for all non-hydrogen atoms (Tables 1-9). Calculations were carried out with an Eclipse S/200 (for II) and a PDP 11/23-Plus (for III and IV) computer using the INEXTL and SDP program packages respectively.

$\text{Cp}_2\text{Cr}_2(\mu\text{-SCMe}_3)(\mu_3\text{-S})_2\text{Fe}(\mu_3\text{-S})_2\text{Fe}_2(\text{CO})_6$ (II)

A solution of $\text{Cp}_2\text{Cr}_2(\mu\text{-SCMe}_3)_2\text{S}$ (0.60 g, 1.35 mmol) and of $\text{Fe}_3\text{S}_2(\text{CO})_9$ (0.65 g, 1.35 mmol) in benzene (35 ml) was kept for 6 h at 20°C under UV irradiation (PRK-4 lamp). The resulting brown-green solution obtained was chromatographed on Al_2O_3 (4 × 15 cm); the red (unchanged $\text{Fe}_3(\text{CO})_9\text{S}_2$) and the brown-green zones were eluted by hexane and benzene respectively. The brown-green solution was concentrated to 15 ml (60°C/0.1 torr), 8 ml of heptane was added, and the solution was then concentrated to 10 ml and cooled to -5°C. The precipitated brown-green prisms were washed with pentane and dried in vacuo. Yield 0.15 g (13%). IR spectrum (ν , cm^{-1}): 810m, 1010w, 1140m, 1940s, 1960s, 1985s, 2010s, 2045s, 2900w, 3080w.

Table 9

Bond angles (in degrees) in $(C_5H_5)_2Cr_2(\mu\text{-SCMe}_3)(\mu_3\text{-S})_2Rh(\mu_3\text{-S})_2Fe_2(CO)_6$ (IV)

Angle	ω	Angle	ω
Fe(1)RhFe(2)	78.2(1)	S(1)Fe(1)S(2)	81.4(3)
Fe(1)RhCr(1)	151.4(2)	S(1)Fe(1)C(1)	100(1)
Fe(1)RhCr(2)	119.5(1)	S(1)Fe(1)C(2)	161(2)
Fe(1)RhS(1)	53.8(2)	S(1)Fe(1)C(3)	87(2)
Fe(1)RhS(2)	53.1(2)	S(2)Fe(1)C(1)	97.8(9)
Fe(1)RhS(3)	101.1(3)	S(2)Fe(1)C(2)	92(2)
Fe(1)RhS(4)	151.8(2)	S(2)Fe(1)C(3)	159(1)
Fe(2)RhCr(1)	119.2(1)	C(1)Fe(1)C(2)	99(1)
Fe(2)RhCr(2)	149.9(2)	C(1)Fe(1)C(3)	102(1)
Fe(2)RhS(1)	53.3(2)	C(2)Fe(1)C(3)	93(1)
Fe(2)RhS(2)	53.3(2)	RhFe(2)S(1)	55.2(2)
Fe(2)RhS(3)	153.3(3)	RhFe(2)S(2)	54.8(2)
Fe(2)RhS(4)	99.2(3)	RhFe(2)C(4)	103.3(7)
Cr(1)RhCr(2)	57.2(1)	RhFe(2)C(5)	107.4(8)
Cr(1)RhS(1)	116.2(2)	RhFe(2)C(6)	144(2)
Cr(1)RhS(2)	155.3(3)	S(1)Fe(2)S(2)	81.6(3)
Cr(1)RhS(3)	52.7(3)	S(1)Fe(2)C(4)	156.3(8)
Cr(1)RhS(4)	53.3(2)	S(1)Fe(2)C(5)	89.0(9)
Cr(2)RhS(1)	156.8(2)	S(1)Fe(2)C(6)	104(1)
Cr(2)RhS(2)	115.5(2)	S(2)Fe(2)C(4)	93.9(8)
Cr(2)RhS(3)	52.9(3)	S(2)Fe(2)C(5)	162.2(9)
Cr(2)RhS(4)	53.2(3)	S(2)Fe(2)C(6)	98(2)
S(1)RhS(3)	104.6(2)	C(4)Fe(2)C(5)	89(1)
S(1)RhS(4)	144.4(2)	C(4)Fe(2)C(6)	101(1)
S(2)RhS(3)	145.6(2)	C(5)Fe(2)C(6)	99(1)
S(2)RhS(4)	102.7(3)	RhCr(1)Cr(2)	61.3(1)
S(3)RhS(4)	93.4(3)	RhCr(1)S(3)	53.5(2)
RhFe(1)S(1)	55.0(2)	RhCr(1)S(4)	53.1(3)
RhFe(1)S(2)	55.0(2)	RhCr(1)S(5)	115.2(3)
RhFe(1)C(1)	141.9(9)	Cr(2)Cr(1)S(3)	54.7(2)
RhFe(1)C(2)	107(2)	Cr(9)Cr(1)S(4)	54.9(2)
RhFe(1)C(3)	104.1(9)	Cr(2)Cr(1)S(5)	56.5(3)
S(3)Cr(1)S(4)	94.0(3)		
S(3)Cr(1)S(5)	76.5(3)	RhS(2)Fe(1)	72.0(2)
S(4)Cr(1)S(5)	100.0(3)	RhS(2)Fe(2)	71.8(2)
RhCr(2)Cr(1)	61.5(1)	Fe(1)S(2)Fe(2)	96.9(3)
RhCr(2)S(3)	53.6(2)	RhS(3)Cr(1)	73.7(3)
RhCr(2)S(4)	53.3(3)	RhS(3)Cr(2)	73.6(3)
RhCr(2)S(5)	116.6(3)	Cr(1)S(3)Cr(2)	70.5(3)
Cr(1)Cr(2)S(3)	54.7(2)	RhS(4)Cr(1)	73.6(3)
Cr(1)Cr(2)S(4)	55.1(2)	RhS(4)Cr(2)	73.6(3)
Cr(1)Cr(2)S(5)	57.9(3)	Cr(1)S(4)Cr(2)	70(3)
S(3)Cr(2)S(4)	94.1(3)	Cr(1)S(5)Cr(2)	65.8(3)
S(3)Cr(2)S(5)	77.1(3)	Fe(1)C(1)O(1)	174(3)
S(4)Cr(2)S(5)	101.2(3)	Fe(1)C(2)O(2)	176(3)
RhS(1)Fe(1)	71.1(3)	Fe(1)C(3)O(3)	175(2)
RhS(1)Fe(2)	71.6(2)	Fe(2)C(4)O(4)	175(3)
Fe(1)S(1)Fe(2)	96.1(3)	Fe(2)C(5)O(5)	177(3)
		Fe(2)C(6)O(6)	179(3)

Table 10
Main geometric parameters of the heterometallic metallocpirane clusters ($\text{RC}_5\text{H}_4)_2\text{Cr}_2(\mu\text{-SCMe}_3)(\mu_3\text{-S})_2\text{M}(\mu_3\text{-S})_2\text{Fe}_2(\text{CO})_6$ ($\text{M} = \text{Fe, Co, Rh}$)

Molecule	Bond lengths (Å) and angles (°)							
	Cr-Cr	Cr-M	Fe-Fe	Fe-M	Cr- μ_3 -S	M- μ_3 -S	Fe- μ_3 -S	Cr ₂ M/MFe ₂
$\text{Cp}_2\text{Cr}_2(\mu\text{-SCMe}_3)(\mu_3\text{-S})_2\text{Fe}(\mu_3\text{-S})_2\text{Fe}_2(\text{CO})_6$	2.610	2.717	2.503	3.018	2.281-2.307	2.245-2.286	2.295-2.309	106.8
$(\text{MeC}_5\text{H}_4)_2\text{Cr}_2(\text{SCMe}_3)(\mu_3\text{-S})_2\text{Co}(\mu_3\text{-S})_2\text{Fe}_2(\text{CO})_6$	2.598	2.629	3.399	3.032	2.538	2.281-2.282	2.182-2.198	2.248-2.250
$\text{Cp}_2\text{Cr}_2(\text{SCMe}_3)(\mu_3\text{-S})_2\text{Rh}(\mu_3\text{-S})_2\text{Fe}_2(\text{CO})_6$	2.608	2.720	3.344	2.650	2.554	2.259-2.270	2.182-2.198	90
		2.724		2.650		2.272-2.294	2.230-2.261	129.1

Table 11

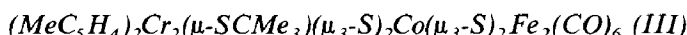
Non-bonded contacts in II and IV (the shortest contacts are given)

Mole- cule	Metal Framework	Intramolecular contacts (Å)			Intermolecular contacts (Å)	
		S...S (Fe ₂ (S) ₂ M)	S...S (Cr ₂ (S) ₂ M)	S...S (CrSMSFe)	O...O (Fe-CO...OCFe)	O...C(Cp) (Fe-CO...CpCr)
III	Cr ₂ (μ ₃ -S) ₂ - Co(μ ₃ -S) ₂ Fe ₂	2.904	3.326	2.763	3.451	3.210
IV	Cr ₂ (μ ₃ -S) ₂ - Rh(μ ₃ -S) ₂ Fe ₂	2.926	3.315	3.620	2.940	3.355

Table 12

Crystal data for (RC₅H₄)₂Cr₂(μ-SCMe₃)(μ₃-S)₂M(μ₃-S)₂Fe₂(CO)₆ (M = Fe, Co, Rh)

	Cp ₂ Cr ₂ (SCMe ₃)(μ ₃ -S)- Fe(μ ₃ -S) ₂ Fe ₂ (CO) ₆ (II)	(MeC ₅ H ₄) ₂ Cr ₂ (SCMe ₃)- (S) ₂ Co(μ ₃ -S) ₂ Fe ₂ (CO) ₆ (III)	Cp ₂ Cr ₂ (SCMe ₃)- (S) ₂ Rh(S) ₂ Fe ₂ - (IV)
System	Triclinic	Orthorhombic	Monoclinic
Space group	P̄1	Pnam	P2 ₁ /n
a, Å	9.691(4)	14.549(2)	9.800(2)
b, Å	12.294(3)	14.480(2)	12.983(3)
c, Å	14.515(5)	14.146(2)	22.606(5)
α, (°)	66.25(2)	90	90
β, (°)	74.89(3)	90	97.05(2)
γ, (°)	78.61(3)	90	90
V, Å ³	1519.8	2980.1	2854.3
Z	2	4	4
2θ _{max}	52	56	56
Number of reflections measured	5032	3032	3174
Number of reflections with I > 3σ(I) used in the refinement	3586	1497	1950
R ₁	0.058	0.037	0.078
R _w	0.074	0.049	0.087



A solution of (MeC₅H₄)₂Cr₂(μ-SCMe₃)(μ₃-S)₂Co(CO)₂ (0.31 g, 0.58 mmol) and of Fe₂S₂(CO)₆ (0.40 g, 1.16 mmol) benzene (35 ml) was kept at 45 °C for 2 h under UV irradiation (PRK-4 lamp). The solvent was evaporated from the reaction mixture at 40 °C/0.1 torr. The initial reagents and the product were extracted by pentane and benzene respectively. The product was crystallized from the benzene/heptane mixture at +5 °C. Single crystals suitable for the X-ray diffraction study were obtained by slow evaporation of the solvent from a solution of the product in a CH₂Cl₂/heptane mixture (1/1). Yield 75%. IR spectrum (ν , cm⁻¹): 530m, 560m, 575m, 810w, 870w, 1015w, 1055vw, 1100w, 1370m, 1440b.m, 1476m, 1615m, 1650w, 1960 sh.v.s, 1970v.s., 2015v.s, 2050s, 2840br w, 2900br.w, 2980br.w, 3120br.w.

Cp₂Cr₂(μ-SCMe₃)(μ₃-S)₂Rh(μ₃-S)₂Fe₂(CO)₆ (IV)

The orange-red solution of Cp₂Cr₂(μ-SCMe₃)(μ₃-S)₂Rh(π-C₈H₁₂) (0.18 g, 0.3 mmol) and of Fe₂S₂(CO)₆ (0.22 g, 0.64 mmol) in benzene (20 ml), was kept for 9 h at 45°C under UV irradiation until it finally became stable chocolate-brown in colour. The solvent was then evaporated at 30°C/15 torr to give a brown oily product which gave at adding of pentane a red-brown solution A * containing the initial reagents and fine, dark-brown crystals.

The crystals were isolated, washed with pentane and dissolved in 10 ml of THF, after the addition of 5 ml of heptane it was kept at -15°C for 3 days. The large, brown prisms that separated were isolated, washed with hexane and dried in vacuo. Yield 0.11 g. IR spectrum (ν , cm⁻¹): 475m, 555s, 595v.s, 810s, 1010w, 1020w, 1065w, 1150m, 1430m, 1955v.s, 1995s, 2020v.s, 2050s, 2900w.

References

- 1 A.A. Pasynskii, I.L. Eremenko, Sov. Sci. Rev. B. Chem., 10 (1988) 443.
- 2 V.W. Day, D.A. Lesch, T.B. Rauchfuss, J. Am. Chem. Soc., 104 (1982) 1290.
- 3 I.L. Eremenko, B. Orazsakhatov, A.S. Abdullaev, S.B. Katser, V.E. Shklover, Yu.T. Struchkov, Zh. Vsesouznogo Khimicheskogo Obshchestva, Vol. XXXII, (1987) 109.
- 4 A.L. Bykovets, O.V. Kuzmin, V.M. Vdovin, A.Ya. Sideridu, G.G. Aleksandrov, Yu.T. Struchkov, Izv. Akad. Nauk SSSR, Ser. Khim., (1981) 490.
- 5 J.A. Kovacs, J.K. Bashkin, R.H. Holm, Polyhedron, 6 (1987) 1445.
- 6 J.H. Van Vleck, The Theory of Electronic and Magnetic Susceptibilities, Oxford Univ. Press, London, 1932.
- 7 R.D. Barr, M. Green, K. Marsden, F.G.A. Stone, P. Woodward, J. Chem. Soc., Dalton Trans., (1983) 507.
- 8 A.A. Pasynskii, I.L. Eremenko, V.R. Zalmanovitch, V.V. Kaverin, B. Orazsakhatov, V.M. Novotortsev, O.G. Ellert, A.I. Yanovsky, Yu.T. Struchkov, J. Organomet. Chem., 356 (1988) 570.
- 9 D.L. Stevenson, C.H. Wei, L.F. Dahl, J. Am. Chem. Soc., 93 (1971) 6027.
- 10 A.A. Pasynskii, I.L. Eremenko, Yu.V. Rakitin, V.M. Novotortsev, V.T. Kalinnikov, G.G. Aleksandrov, Yu.T. Struchkov, J. Organomet. Chem., 165 (1979) 57.
- 11 W. Hieber, J. Gruber, Z. Anorg. Allg. Chem. B, 296 (1958) 91.
- 12 A.A. Pasynskii, I.L. Eremenko, Yu.V. Rakitin, V.M. Novotortsev, O.G. Ellert, V.T. Kalinnikov, V.E. Shklover, Yu.T. Struchkov, S.V. Lindeman, T.Kh. Kurbanov, G.Sh. Gasanov, J. Organomet. Chem., 248 (1983) 309.
- 13 A.A. Pasynskii, I.L. Eremenko, B. Orazsakhatov, G.Sh. Gasanov, V.M. Novotortsev, O.G. Ellert, Z.M. Seifulina, V.E. Shklover, Yu.T. Struchkov, J. Organomet. Chem., 270 (1984) 53.
- 14 V.M. Novotortsev, Dr.Ph. Thesis, Moscow, 1974.

* Along with IV the violet crystals of the previously identified complex QRh(CO)₂ [8] were isolated from solution A and characterized by TLC and IR spectroscopy (ν (CO), cm⁻¹: 2025vs, 1965vs).